IMAGE BACKLIGHT COMPENSATION USING RECURRENT FUNCTIONAL NEURAL FUZZY NETWORKS BASED ON MODIFIED DIFFERENTIAL EVOLUTION

S. C. YANG, C. J. LIN, H. Y. LIN, J. G. WANG AND C. Y. YU

Abstract. In this study, an image backlight compensation method using adaptive luminance modification is proposed for efficiently obtaining clear images. The proposed method combines the fuzzy C-means clustering method, a recurrent functional neural fuzzy network (RFNFN), and a modified differential evolution. The proposed RFNFN is based on the two backlight factors that can accurately detect the compensation degree. According to the backlight level, the compensation curve function of a backlight image can be adaptively adjusted. In our experiments, six backlight images are used to verify the performance of proposed method. Experimental results demonstrate that the proposed method performs well in backlight problems.

1. Introduction

Improper setups of exposure parameters or the object located between the light source and camera without enough lights projected will lead to the backlight images in which the object is hardly identified compared to the surrounding. In order to tackle this problem, the spatial information around the object and the statistic information of related pixels such as histogram equalization (HE) and histogram specification (HS) are often utilized. The histogram here means the frequency distribution of luminance which is spatial statistic information. Some modified models like global histogram equalization (GHE) and local histogram equalization (LHE) were most adopted methods to solve backlight problem. However, most histogram equalization methods often produced side effects at the edges of a backlight object and its surrounding areas. An smart contrast enhancement approach, based on conventional histogram equalization and dynamic histogram equalization (DHE), was applied to partition the image histogram by local minima and to assign specific gray-level ranges for each partition [15]. Unfortunately, this method cannot focus on the backlight area owing to it only extracted the histogram information by applying histogram equalization to the luminance frequency distribution [2, 6, 8]. It is the same that such information cannot further deal backlight cases well for preventing interference in non-backlight area. Recently, an Adaptive Inverse Hyperbolic Tangent (AIHT) algorithm [19] was proposed to improve the display quality and

Received: July 2013; Revised: November 2015; Accepted: July 2016

Key words and phrases: Neural fuzzy network, Recurrent network, Differential evolution, Fuzzy c-means, Backlight compensation, Contrast enhancement.

contrast of a scene. The proposed AIHT determines the contrast levels of an original image as well as parameter space for different contrast types so that not only the original histogram shape features can be preserved, but also the contrast can be enhanced effectively. Several modified AIHT methods [7, 17, 18] were also proposed to improve backlight problems. In addition, Huang et al. [5] applied the just noticeable difference theory and decomposed an image into a human visual system (HVS) response layer and a background luminance layer to improve local contrast. Therefore, an adaptive and novel enhancement approach depending different backlight degrees is generally required for achieving better processed solution.

In literature, several techniques of classification and clustering have been proposed to support these required segmentation. Chen et al. [1] proposed a two-stage processing method which utilized the fuzzy C-means to segment the backlight image into portions of main object and related background, as well as compensated the contrast of the object by a fuzzy inference model. One of the advantages of such an approach is that it is able to compensate the object independently without interfering its surrounding area. In addition, some nonlinear system identification models were frequently applied as well, while the most common model is based on neural networks or neural fuzzy networks. In [4], adaptive fuzzy systems were proposed for many applications. Then, [3, 9] proposed adaptive neuro-fuzzy systems for controlling and modeling, as well as other relative works in [10, 20] for clustering and identification. However, Chen et al. [1] proposed a recurrent functional-link-based neural fuzzy system for the prediction of time sequence and skin color detection. Such a model can solve the temporal sequence processing problem effectively and has superior performance than traditional artificial neural networks (ANN) or fuzzy inference systems (FIS).

In addition, there are many applications of evolutionary computation in engineering problems, such as GA, PSO and DE. Paterlini [12] compared the performance of GAs for a representative point evolution approach to clustering with the particle swarm optimization (PSO) and DE, which the differential evolution (DE) algorithm is one of the most efficient optimization methodologies. Storn and Price [14] demonstrated that DE converges faster and with higher certainty than many other acclaimed global optimization methods. Afterwards, we found that DE-based approaches have been applied with FIS, ANN or both in many areas [13]. According to the above-mentioned description, we can get better adaptability parameters and as curve of a compensation factor to adjust the backlight image by using DE algorithm. In summary, under the fact that constructing a model by applying modifications to DE can quickly complete the optimal parameters setup for backlight compensation, in this paper we proposed a recurrent functional neural fuzzy network to combine with the modified DE method in order to effectively improve the efficiency in parameters optimization. Experimental results show that our proposed scheme can effectively recover backlight images to an acceptable level, as well as surrounding contrast.

The rest of this paper is organized as follows. First, the theoretical background and the structure of the recurrent functional-link-based neuro-fuzzy network (RFNFN) are described in section 2. Next, differential evolution (DE) and

the modified model are introduced in section 3. Then, the whole backlight image processing procedure including the model used and the parameter optimization will be demonstrated by a flow chart and detailed explanation in section 4. In section 5 shows experimental results as well as comparisons with some existing algorithms by quantitative measures of image quality. The discussions about our implementation conclude this work in section 6.

2. **A Recurrent Functional Neural Fuzzy Network**

The architecture of recurrent functional-link-based neural-fuzzy network (RFNFN) is described in this section. In practice, the FLNFN proposed by [1] utilizes a fuzzy if-then rule in the following form.

$$\begin{aligned} \textit{Rule-}j\text{:} \quad & \text{IF } h_{1j} \text{ is } A_{1j},\ h_{2j} \text{ is } A_{2j},\ \cdots,\ h_{ij} \text{ is } A_{ij},\ \cdots, \text{ and } h_{Nj} \text{ is } A_{Nj} \\ & \text{THEN } \hat{y}_j = \sum_{k=1}^{M} w_{kj}\phi_k = w_{1j}\phi_1 + w_{2j}\phi_2 + \ldots + w_{kj}\phi_k, \end{aligned} \tag{1}$$

where $i = 1, 2, \cdots, N$, $h_{ij}u_i^{(1)}(t) + u_i^{(2)}(t-1) \cdot \theta_{ij}$, $\hat{y}_j$ is local output, A_{ij} is the linguistic term of the precondition part with the Gaussian membership function, N is the number of input variables, w_{ij} is the linked weight of the local output, ϕ_k is the basis trigonometric function of the input variables, M is the number of basis functions, and *Rule-j* represents the j^{th} fuzzy rule. In other words, the input of each membership function is the summation of input x_i and the temporal term $u_{ij}^{(2)} \cdot \theta_{ij}$. Moreover, as shown in Fig. 1, the recurrent mechanism of outputs in layer 2 is embedded for temporal memory. There are five layers in our proposed RFNFN model, while for convenience two inputs in layer one, three fuzzy inference rules, and one output are depicted as in Fig. 1.

It is obvious that the fuzzy system with temporal terms, i.e. the feedback inputs, can be considered as a dynamic FIS having recurrent memory. In the following, the detailed descriptions of the transfer function and calculation for each layer of the RFNFN are presented. Note that $u^{(l)}$ denotes the output of the layer l.

Layer 1 **(Input Node):** The output of each node in this layer is as same as its corresponding input. In other words, nodes in this layer transmit their inputs directly to form the outputs as

$$u_i^{(1)} = x_i. \tag{2}$$

Layer 2 **(Input Term Node):** The nodes in this layer represent linguistic labels of the input variables in Layer 1, while the temporal memory is the degree specified by the membership function. We adopt the Gaussian membership function to perform the transformation as

$$u_{ij}^{(2)} = exp\left(-\frac{[h_{ij} - m_{ij}]^2}{\sigma_{ij}^2}\right), \tag{3}$$

where m_{ij} and σ_{ij} are the mean and variance of Gaussian membership function of the j^{th} term of the i^{th} input variable x_i, respectively. In addition, the recurrent

operation of inputs with respect to the discrete time t is defined by

$$u_{ij}^{(2)}(t) = u_i^{(1)}(t) + u_{ij}^{(2)}(t-1) \cdot \theta_{ij}, \tag{4}$$

where $u_{ij}^{(2)}(t-1)$ means the output from layer 2 at previous time step. This term will feedback the memory which stores the past information and θ_{ij} denotes the linking weight from i^{th} node in layer 2 to j^{th} node in layer 3.

Layer 3 **(Rule Node):** This layer represents the preconditioned part of a fuzzy logic rule. The nodes receive membership degrees of the associated rules from the nodes in layer 2. Then we apply the product operator to perform the IF-condition matching calculation of the fuzzy rules. Such an output from a node in layer 3 can be described as

$$u_j^{(3)} = \prod_i u_{ij}^{(2)}, \tag{5}$$

in which $u_j^{(3)}$ is the corresponding firing strength of the j^{th} rule in layer 3.

Layer 4 **(Consequent Node):** Comparing to the ones in layer 3, nodes in this layer are called consequent nodes. There will be other nonlinear combinations of input variables from a functional link-based neural network to multiple with the outputs from layer 3, as the following relationship for outputs of layer 4,

$$u_j^{(4)} = u_j^{(3)} \cdot \sum_{k=1}^{M} w_{kj}\phi_k, \tag{6}$$

where w_{kj} is the corresponding linking weight in the functional link based neural network and ϕ_k is the functional transform of inputs. We apply a set of trigonometric basis functions as a vector given by

$$\begin{aligned} \Phi &= [\phi_1, \phi_1, \cdots, \phi_M] \\ &= [x_1, sin(\pi x_1), \cos(\pi x_1), x_2, \sin(\pi x_2), \cos(\pi x_2)], \end{aligned} \tag{7}$$

where $M = 6$ for two input variables. Hence M is the dimension number of basis functions, i.e., $M = 3 \times N$ and N is the number of input variables.

Layer 5 **(Output Node):** This is the last layer of this model for producing system outputs. Within this layer outputs of nodes in layer 4 will be calculated as a defuzzify function. The transfer function will utilize the concept of the COA (center of area) as

$$y = u^{(5)} = \frac{\sum_{j=1}^{R} u_j^{(4)}}{\sum_{j=1}^{R} u_j^{(3)}} = \frac{\sum_{j=1}^{R} \left(u_j^{(3)} \cdot \sum_{k=1}^{M} w_{kj}\phi_k \right)}{\sum_{j=1}^{R} u_j^{(3)}}, \tag{8}$$

where R is the number of fuzzy rules and y represents the system output of the RFNFN model.

3. The Proposed Learning Method

The proposed learning method for searching the optimal parameters of the RFNFN is the modified differential evolution (MODE), which is based on the basic DE. An MODE is designed for applying to our RFNFN model in order to infer the backlight degree of the target images.

3.1. **Review of Differential Evolution.** This subsection describes basic concepts of differential evolution (DE). Differential evolution is a parallel direct search method which utilizes N-dimensional parameter vectors as a population for each generation G.

$$x_{i,G}, i = 1, 2, \cdots, NP. \tag{9}$$

The initial each dimensional is chosen randomly and should cover the entire parameter space for each population. For the DE generates new parameter vector by adding the weighted difference between two population vectors to a third vector, which let this operation be called "mutation". The mutated vectors parameters are then mixed with the parameters of another predetermined vector, the target vector, to yield the so-called trial vector. The situation of parameter mixed is often referred to as "crossover" will be explained later in more detail. If the trial vector yields a lower cost function value than the target vector, the trial vector replaces the target vector in the following generation. This last operation is called "selection". Each population vector has to serve once as the target vector so that NP competitions take place in one generation. The strategies of three step can be described as follows:

Step1: (Mutation): For each target vector $x_{i,G}, i = 1, 2, \cdots, NP$ is computed and a new mutant vector is generated according to

$$v_{i,G+1} = x_{r_1,G} + F \cdot (x_{r_2,G} - x_{r_3,G}), \tag{10}$$

where random indexes $r_1, r_2, r_3 \in \{1, 2, \cdots, NP\}$. The randomly chosen integers r_1, r_2 and r_3 are also chosen to be different from the running index i, so that NP must be greater or equal to four to allow for this condition. F is a constant factor and the parameter $\in [0, 1]$ which controls the amplification of the differential variation $(x_{r_2,G} - x_{r_3,G})$. Present a two-dimensional example to illustrate operation of the different vectors in Fig 2.

Step2: (Crossover): In order to increase the diversity of the perturbed parameter vectors, crossover is introduced as follows:

$$u_{i,G+1} = (u_{1i,G+1}, u_{2i,G+1}, \cdots, u_{Ni,G+1}), \tag{11}$$

where

$$u_{ji,G+1} = \begin{cases} v_{ji,G+1} & \text{if } (r(j) \leq CR) \text{ or } j = rn(i) \\ x_{ji,G+1} & \text{if } (r(j) > CR) \text{ or } j \neq rn(i) \end{cases}, \ j = 1, \cdots, N \tag{12}$$

In Eq. (12), $r(j)$ is the j^{th} evaluation of a uniform random number and the value is between 0-1. CR is the crossover constant $\in [0, 1]$ which has to be determined by the user. $rn(i)$ is a randomly chosen index $\in 1, 2, \cdots, N$ which ensures that $u_{i,G+1}$ gets at least one parameter from $v_{i,G+1}$. A simple example of operation described as shown in Fig 3.

Step3: (Selection): If vector $u_{i,G+1}$ yields a smaller cost function value than $x_{i,G}$, then $x_{i,G+1}$ is set to $u_{i,G}$; otherwise, the old value $x_{i,G}$ is retained.

3.2. **The Proposed Modified Differential Evolution.** As illustrated in Fig. 4, the proposed MODE algorithm consists of four phases, i.e., the phases of initialization, evaluation, reproduction and crossover, while the detailed descriptions of these phases are presented as follows:

A. Initialization Phase

Initializing population contains a set of many feasible solutions, i.e., individuals, for the RFNFN in multidimensional space. All parameters of the RFNFN are coded as shown in Fig. 5. It illustrates an example of coding of the RFNFN parameters as an individual in the population. In Fig. 5 , index i indicates the i^{th} input variable, and index j is for the j^{th} rule. In this work, we adopt the Gaussian membership function with the mean m_{ij} and the variance σ_{ij} in the layer 2 of the RFNFN. Then, w_{ij} is the corresponding linking weight of the consequent part that is connected to the j^{th} rule node. There are two ways to encode the individuals, i.e., binary and real number. Real number encoding is applied to each individual and each element is generated randomly in the range of $[-1, 1]$.

B. Evaluation Phase

While the population is generated, the performance of each individual is evaluated by the fitness function or the objective function. Owing to the single output in our backlight compensation, we adopt the mean squared error of model output and target output as:

$$F = \frac{1}{N_o} \left(y_k - \overline{y}_k \right)^2 , \tag{13}$$

where y_k represents the model output, $\overline{y}_k$ is the desired output, N_o is the number of output, and k is the k^{th} output of the model.

C. Reproduction Phase

After the performance of each individual is evaluated, the best individual x_{best} can be selected by permutation in each iterations. Then in the g^{th} iteration, the i^{th} individual $x_{i,g}$ is taken as one of patent and three other individuals, i.e., $x_{r_1,g}, x_{r_2,g}, x_{r_3,g}, r_1 \neq r_2 \neq r_3$, are selected randomly except $x_{i,g}$. A new individual is generated by modified difference of $x_{r_1,g}, x_{r_2,g}, x_{r_3,g}$ and $x_{best,g}$ as defined by Eq. (14).

$$v_{i,g} = x_{r_1,g} + (1 - f) \times (x_{r_2,g} - x_{r_3,g}) + f \cdot (x_{best,g} - x_{r_1,g}), \tag{14}$$

where f is commonly known as a scaling factor and is defined as g/N, and N is the total number of iteration. The portion of direction will rise up in proportion to the iteration and then this new individual $v_{i,g}$ becomes another patent.

D. Crossover Phase

A new offspring individual $u_{i,g}$ will be generated by $x_{i,g}$ and $v_{i,g}$. The element of $u_{i,g}$ in the reproduction phase inherited from $x_{i,g}$ and $v_{i,g}$ is determined by a crossover probability CR which will be set up in the range of [0, 1] beforehand. The elements of the patent, i.e., $x_{i,g}$ and $v_{i,g}$, will crossover into the offspring $u_{i,g}$.

$$u_{i,g} = \begin{cases} v_{id,g} & \text{if } rand(d) \leq CR \\ x_{id,g} & \text{if } rand(d) > CR \end{cases} \tag{15}$$

where $d = 1, 2, 3, \cdots, D$ denotes the d^{th} element of the individual, D is the total amount of the element, and $rand(d)$ represents the d^{th} random number. Fig. 6 depicts the process of a crossover example of 8-dimensional parameters.

The survival selection is applied to decide whether $x_{i,g}$ can survive to the next iteration. Each fitness of $x_{i,g}$ and $v_{i,g}$ is evaluated according to the Eq. (13). The

winner is promoted to the population in next generation as the following:

$$x_{i,g+1} = \begin{cases} u_{i,g} & \text{if } u_{i,g} \leq x_{i,g} \\ x_{i,g} & \text{if } u_{i,g} > x_{i,g} \end{cases} . \tag{16}$$

4. Backlight Image Processing

The main procedure of backlight image processing is illustrated as shown in Fig. 7. There are two processes for contrast compensation, i.e., processes of training and testing. In the training process a RFNFN will extract the backlight information, while the well-trained parameters can be utilized for identifying the other testing images in testing process. In the following sub-sections, detailed procedures and descriptions of image color-space transformation, factors of the backlight image, and image compensation curve are presented, respectively.

A. Image Color Space Transformation

In general, the color space of an image depends on its file format, while the RGB color space is the most popular one in image processing. Aiming to process the important elements of backlight, brightness or luminance, we will transform the RGB color space into the YIQ color space. The component Y in YIQ represents the luminance of the target images and will be adopted for further processing without destroy any original color, by considering the fact that human eyes are less sensitive to quantified error of the chrominance of the image. When the color space transforms from RGB into YIQ, the transformation equation is defined as

$$\begin{bmatrix} Y \\ I \\ Q \end{bmatrix} = \begin{bmatrix} R \\ G \\ B \end{bmatrix} \begin{bmatrix} 0.299 & 0.587 & 0.114 \\ 0.596 & -0.275 & -0.321 \\ 0.212 & -0.523 & 0.311 \end{bmatrix} \tag{17}$$

B. Factors of the Backlight Image

There are two backlight factors, i.e. *B_fcm* and *B_hist*, used to evaluate the backlight level which will decide coefficient of luminance function. Since different combinations of *B_fcm* and *B_hist* generally have many divergent inferences of backlight, we will apply a fuzzy model to tackle this situation, while the details of such a model are presented as in the following paragraphs.

(a) Backlight Factor *B_hist*

When referring to a backlighted image, it often indicates that the contrast between an object and its background is very large. In general, the luminance of the object that we are interested is lower than that of its background. Figure 8 presents an example of a backlighted image.

Figure 9 shows another backlighted example of the histogram of luminance. It can be clearly observe that the distribution between the object and its surrounding background has an obvious gap which separates the histogram into two different groups.

In such a case, we shall utilize a sliding window (SW) to calculate the *B_hist* factor which measures the gradient between the object and background in the de-cumulative frequency histogram (Fig. 10). The de-cumulative frequency distribution of luminance defines the ratio of the number of pixels whose brightness is

greater than the threshold over the whole amount of pixels in the image. In practice, we take the duration of de-cumulative frequency equals or smaller than 0.2 along the span of luminance to calculate the maximum SW, while Fig. 10 depicts the relationship between the luminance and de-cumulative frequency, and the usage of the SW.

As the positive relation observed from many backlight images, we find that backlight degree rises with the maximum SW. Consequently, the *B_hist* can be calculated through

$$B_hist = T_{hist}\left(\frac{SW_{max}}{255}\right), \tag{18}$$

where $T_{hist}(\bullet)$ transforms the *B_hist* into a fuzzy degree, i.e. acting as a transfer function, while the transfer function shown has the following relation:

$$T_{hist}(x) = \begin{cases} (x-0.3)/(0.6-0.3), & \text{if } 0.6 > x > 0.3 \\ 1, & \text{if } x \geq 0.6 \\ 0, & \text{otherwise} \end{cases}. \tag{19}$$

(b) Backlight Factor *B_fcm*

Since the clustering orientation is also an index to distinguish the level of backlight, we apply the fuzzy c-means (FCM) [16] to classify the luminance in the backlighted image processing. This can be easily understood by representing both the light background and dark object. Accordingly, we determine the cluster number to be set to two, and as the result, we will have two clustering centroids, namely C_1 and C_2.

Just as the above descriptions mentioned, the luminance can be accumulated in a histogram between the background and the object. In such a case, the smaller accumulative amount of luminance between the background and the object is, the higher backlight degree will be. Hence, we can define another backlight factor, i.e. *B_fcm*, to calculate the backlight degree of an image as below,

$$B_fcm = T_{fcm}\left(\frac{\sum_{i=C_1}^{C_2} p(r_i)}{(C_2 - C_1) \times \frac{p(C_1)+p(C_2)}{2}}\right), \tag{20}$$

where $p(r_i) = \frac{n_i}{n}$ is the frequency of the i^{th} luminance level, n_i is the amount of pixel for i^{th} luminance appeared, and n is the total amount of all pixels. In Eq. (20), $T_{fcm}(\bullet)$ is also defined as a transfer function which transforms the frequency summation between two FCM centroids into a fuzzy inference. The content of transformation is stated as following,

$$T_{fcm}(x) = \begin{cases} (0.8-x)/(0.8-0.25), & \text{if } 0.8 > x > 0.25 \\ 1, & \text{if } x \geq 0.8 \\ 0, & \text{otherwise} \end{cases}. \tag{21}$$

Backlight factor represents the accumulation of luminance frequency between two FCM cluster centroids, i.e. C_1 and C_2. Those centroids are the centers of background with lighter luminance and object with darker luminance, respectively. When the value of frequency accumulation between these two centroids becomes large, the level of backlight *B_fcm* will raise up as well.

Parameter	Value
Population size	60
Iterations	1000
CF	0.09

TABLE 1. Parameters Setup

(c) Image Compensation Curve

For the purpose of adaptive compensation, a quadratic function curve is referred to be determined by the backlight degree and the centroids of fuzzy c-means. In such a curve, it consists of two curves, i.e., one concave curve and one convex curve, as shown in Fig. 11 and its curve function is expressed as

$$f(x) = \begin{cases} \frac{-b}{a}(x-a)^2 + b, & \text{if } x < a \\ \frac{(255-b)}{(255-a)^2}(x-a)^2 + b, & \text{otherwise} \end{cases}. \tag{22}$$

The turning point (TP) can be adjustable by the coefficients (a , b) as

$$\begin{cases} a = (C_1 + C_2)/2 \\ b = a + [B_{degree} \times (C_2 - a)] \end{cases}, \tag{23}$$

where C_1 and C_2 are the cluster centers obtained from the FCM algorithm and B_{degree} is the backlight degree obtained by the RFNFN.

For each pixel of the backlight image, the luminance is adjusted by its corresponding compensation curve. The final result depends on this curve and the turning point is adaptive, according to the backlight levels of different images.

5. Experimental Results

Images with different types of histogram distributions were tested for experiments. The comparison results include the visual results and the quantitative measures.

5.1. **Comparisons of Visual Results.** The images were taken by a Fuji FinePix S602 digital camera, with the format of 24 bits and 2048*1536 resolutions. Afterward, these images are resized to 640*480 in order to shorten the processing duration. The color space of the preprocessing is the RGB and is transformed into the YIQ as mentioned previously. The Y-element matrix of the image will be singly extracted for further processing. Moreover, the unit formats number of the Y elements will be transformed from double to single, for the sake of convenient calculation.

A. Learning of RFNFN based on MODE

We built a recurrent function neural fuzzy network to compensate the backlight images in this work. There are two inputs in layer one, three fuzzy rules with recurrent input, and a basis function of six dimensions in the model. The setup of parameters is listed in Table 1 and the result of squared error with corresponding iterations is shown in Fig. 12, while the parameters of the trained RFNFN are stored for inferring the backlight degree latter.

B. Backlight Image Compensation

We take several backlight images indoors and outdoors under different conditions of light sources. These backlight images are separated into the following two groups to compare the effectiveness with our proposed process and the histogram equalization.

(A) Group 1

There are four backlight images taken in Fig. 13. Backlight image of "building object" will be discussed. Since the background overexposes, this situation causes the foreground object darkness and unclear. After completing the backlight compensation process, the foreground object is very clear and the contrast of background still maintains good results.

In the original backlight image of the "Under tree", compared to its right-side bright sky, it can be sensed that the surface of leaves is almost dark totally. After completing the backlight compensation process, the branches and the leaves can be clearly identified. This enhancement makes the details of braches and leaves becoming more clearly and without sacrificing any contrast of the bright sky and white cloud. Even so, we can still observe that some leaves around the top left section are not distinct enough, but this does not affect the resulted effects of contrast enhancement. On the other hand, the result of the HE has better enhanced effect and the contrast becomes lower.

Next, in another backlight image "Roof of a building", the inner section of the roof is undetectable. The contrast of the HE processed image is over compensated which emphasizes the luminance of the sky. There is also some block-effect shown beneath the roof. However, the rusted iron bars become very clear after processed by our proposed method and there is no block with over enhancement.

Comparing to previous images with the light vertically projected from the top to the object, an artificial wall stabile with light from right side is also illustrated. The original backlight image "Artificial wall stabile" has the backlight effect in which the light was decreased from right to left and the color of the artificial stabile cannot be identified on the left bottom section at all. The HE compensated image is presented and it is over enhanced in the corresponding background. The presentation of the left bottom section for this method is clearer and the texture on artificial wall stabile is also more identifiable than the unprocessed original image.

(B) Group 2

In this group, we take another three backlight images for further comparative demonstrating of backlight processing. In this case, a book is located on the beaverboard where the light source is located at the back side. The title of the book in the original image is unidentified and there some light sources located from the back top direction. In the HE enhanced image, the compensated image reveals serious block-effect and the problem of over-enhancement. Then the first word of the title of the book "FUZZY" can easily identified after the proposed compensated process, though the word "LOGIC" can only figure out by the shape. It is surprised that a pack of A4 papers in the original image after our backlight processing cannot

Methods \ Test image		Dawn	Afternoon	Park	Airport hall
— Histogram equalization [11]	MSE	0.16913	0.00961	0.05862	0.00206
	SNR	5.0272	46.391	1.6688	175.15
	PSNR	5.9127	104.08	17.060	486.08
— Contrast limited adaptive histogram equalization [21]	MSE	0.0432	0.0432	0.0339	0.0492
	SNR	10.316	10.316	2.8852	7.3229
	PSNR	23.143	23.143	29.495	20.323
— Adaptive inverse hyperbolic tangent [19]	MSE	0.0386	0.0099	0.0034	0.0163
	SNR	22.1137	25.0963	28.8848	22.1386
	PSNR	25.8902	101.170	295.286	61.4400
— AIHT⨁CLAHE [18]	MSE	0.0378	0.0072	0.0026	0.0118
	SNR	23.257	57.731	29.15	23.473
	PSNR	26.138	106.568	301.246	64.179
— 8SAIHT [17]	MSE	0.037	0.0043	0.00248	0.0094
	SNR	23.528	59.825	30.08	23.982
	PSNR	26.197	108.216	302.807	66.704
— Proposed method	MSE	0.03669	0.00114	0.00165	0.00018
	SNR	24.85081	65.664	30.566	25.086
	PSNR	26.286	109.364	305.194	69.674

TABLE 2. Quantitative Analysis of MSE, SNR, and PSNR

be identified clearly. For the second backlighted image the girls face in not clear enough, compared to her white clothes. The HE compensated image cannot modify the backlight on her face. On the other hand, when it is compensated by our proposed process, we can definitely observe the girls face with a lovely smile. This result shows that our process is better than the HE on the outdoor human photography. In the third backlight image "Sunflower", the light source is at left behind and the sunflower is seriously backlighted in Fig 14. The HE compensation has enhanced the sunflower, but the edge effect is obvious which makes the image not so natural. However, our adaptive compensated result can show that the texture of sunflower.

5.2. **Analysis of Quantitative Measurement.** In this subsection, some daily life images with contrast or backlight are analyzed and demonstrated the comparison results. These images are categorized into outdoor and indoor. The outdoor images include dawn and afternoon images whereas the indoor images include park and hall. Figure 15 displays the results of the backlight or contrast image processing by histogram equalization [11], adaptive inverse hyperbolic tangent [19], modulated AIHT image contrast enhancement algorithm based on contrast-limited adaptive histogram equalization (AIHT⨁CLAHE) [18], eight-scale image contrast enhancement based on adaptive inverse hyperbolic tangent algorithm (8SAIHT) [17], and the proposed method. Table 2 shows the quantitative measures of MSE, SNR, and PSNR using various image backlight processing methods. Experimental results show that the proposed method is better than other methods.

6. **Conclusions**

In this study, a novel compensation method is proposed for solving backlight image problems. The proposed method combines the RFNFN with MODE and the multi-quadratic curve for different backlight levels. The RFNFN is based on the two backlight factors that can accurately detect the compensation degree. Images

with different histogram distributions are tested for experiments. The comparison results include the visual results and the quantitative measures. Experimental results demonstrate that the proposed method performs well in backlight image problems.

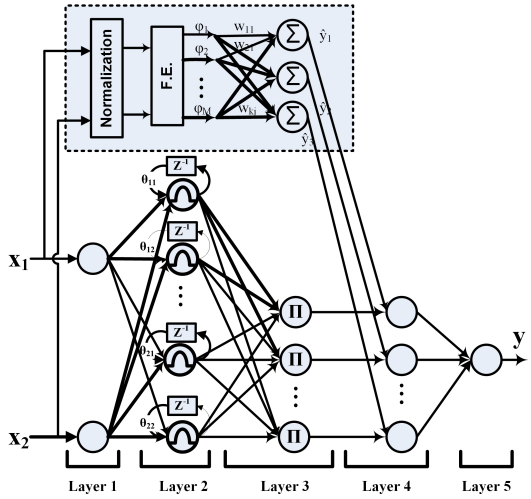


FIGURE 1. Structure of Proposed RFNFN Model

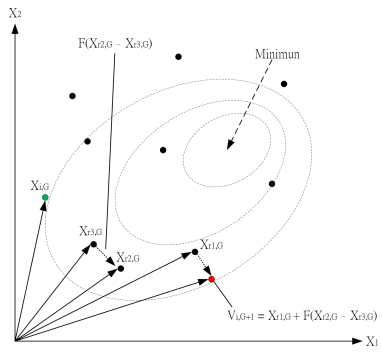


FIGURE 2. An Example of a Two-dimensional Cost Function Showing Its Contour Lines and the Process for Generating $v_{i,G+1}$

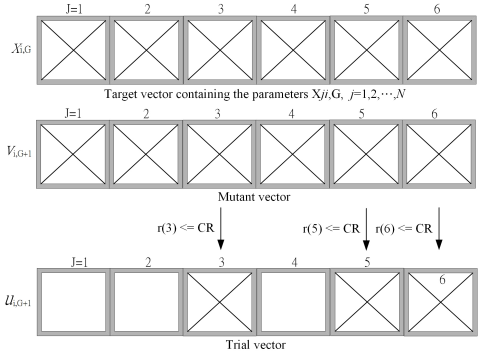


FIGURE 3. Illustration of the Crossover Process for $N = 6$ Parameters

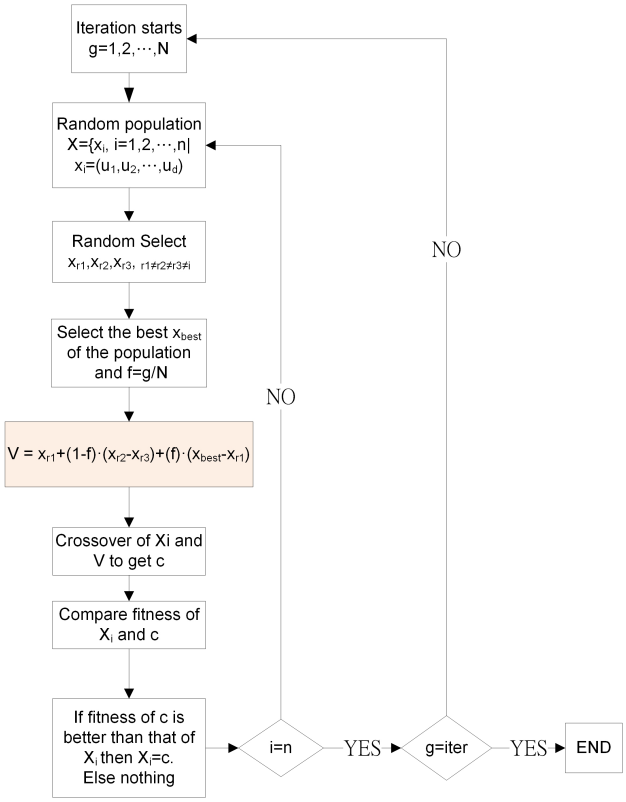


FIGURE 4. Modified Differential Evolution Process

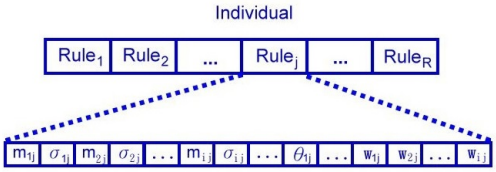


FIGURE 5. Individual Coding of the Proposed MODE

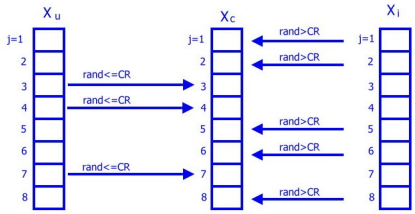


FIGURE 6. The Crossover Operation for 8 Dimensional Parameters

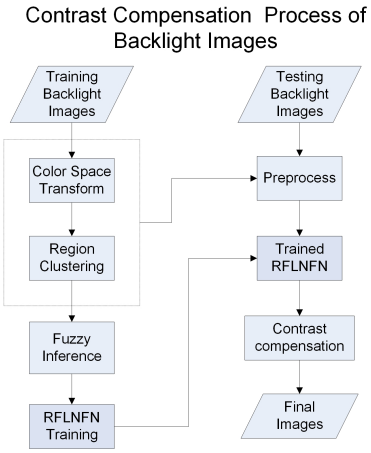


FIGURE 7. Contrast Enhancement Process of Backlight Images



FIGURE 8. An Example Backlight Image

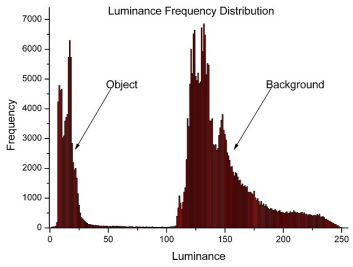


FIGURE 9. Histogram of Luminance for a Backlighted Image

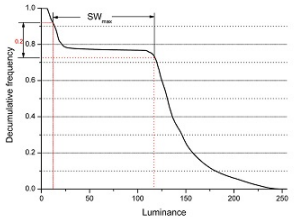


FIGURE 10. De-cumulative Luminance Frequency Histogram of a Backlight Image

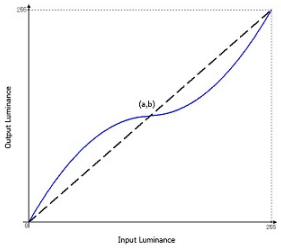


FIGURE 11. Luminance Compensation Curve

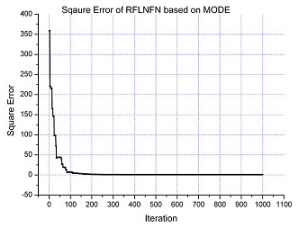


FIGURE 12. Learning Curve of RFNFN Based on MODE

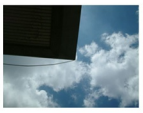
	Building object	Under tree	Roof of a building	Artificial wall stabile
(a)				
(b)				
(c)				

FIGURE 13. Backlight Images Processing: (a) Original backlight Image; (b) HE [11]; (c) Proposed Method

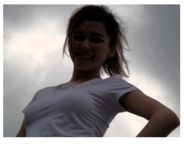
	A book indoor	A smiling girl	Sunflower
(a)			
(b)			
(c)			

FIGURE 14. Backlight Images Processing: (a) Original Backlight Image; (b) HE [11]; (c) Proposed Method



FIGURE 15. Comparison Results of Various Image Backlight Processing Methods: (a) Original Image; (b) HE [11]; (c) Contrast-limited Adaptive Histogram Equalization [21]; (d) Adaptive Inverse Hyperbolic Tangent [19]; (e) AIHT$\bigoplus$CLAHE [18]; (f) 8SAIHT [17]; (g) Proposed Method

References

[1] C. H. Chen, C. J. Lin and C. T. Lin, *A recurrent functional-link-based neural fuzzy system and its applications*, Proceedings of the 2007 IEEE Symposium on Computational Intelligence in Image and Signal Processing (CIISP 2007), (2007), 415-420.

[2] J. Duan and G. Qiu, *Novel histogram processing for colour image enhancement*, Proceedings of the Third International Conference on Image and Graphics (ICIG04), Hong Kong, China, (2004), 55-58.

[3] A. A. Fahmy and A. M. Abdel Ghany, *Adaptive functional-based neuro-fuzzy PID incremental controller structure*, Neural Computing and Applications, **26(**6) (2015), 1423-1438.

[4] M. Hojati and S. Gazor, *Hybrid adaptive fuzzy identification and control of nonlinear systems*, IEEE Transactions on Fuzzy Systems, **10(**2) (2002), 198-210.

[5] T. H. Huang, K. T. Shih, S. L. Yeh and H. H. Chen, Enhancement of backlight-scaled images, IEEE Transactions on Image Processing, **22(**12) (2013), 4587-4597.

[6] H. Kabir, A. Al-Wadud and O. Chae, *Brightness preserving image contrast enhancement using weighted mixture of global and local transformation functions*, The International Arab Journal of Information Technology, **7(4)** (2010), 403-410.

[7] H. Y. Lin, C. Y. Lin, C. J. Lin, S. C. Yang and C. Y. Yu, *A study of digital image enlargement and enhancement*, Mathematical Problems in Engineering, Article ID 825169, (2014).

[8] D. Menotti, L. Najman, J. Facon and A. A. A. de Araujo, *Multi-histogram equalization methods for contrast enhancement and brightness preserving*, IEEE Transactions on Consumer Electronics, **53(**3) (2007), 1186-1194.

[9] A. H. Mohamed, *A genetic based neuro-fuzzy controller system*, International Journal of Computer Applications, **94(**1) (2014), 14-17.

[10] M. Panella and A. S. Gallo, *An input-output clustering approach to the synthesis of ANFIS networks*, IEEE Transaction on Fuzzy Systems, **13(**1) (2005), 69-81.

[11] O. Patel, Y. P. S. Maravi and S. Sharma, *A comparative study of histogram equalization based image enhancement techniques for brightness preservation and contrast enhancement*, Signal & Image Processing: An International Journal (SIPIJ), **4(**5) (2013), 11-25.

[12] T. K. S. Paterlini, *Differential evolution and particle swarm optimization in partitional clustering*, Computational Statics & Data Analysis, **50(**5) (2006), 1220-1247.

[13] A. P. Piotrowski, *Differential evolution algorithms applied to neural network training suffer from stagnation*, Applied Soft Computing, **21**(2014), 382V406.

[14] R. Storn and K. Price, *Differential evolution-A simple and efficient heuristic for global optimization over continuous spaces*, Journal of Global Optimization, **11(**4) (1997), 341-359.

[15] M. A. Wadudx, M. H. Kabir, M. A. A. Dewan and O. Chae, *A dynamic histogram equalization for image contrast enhancement*, IEEE Transactions on Consumer Electronics, **53(2)** (2007), 593-600.

[16] J. Yen and R. Langari, *Fuzzy Logic: intelligence, control, and information*, Prentice Hall, 1998.

[17] C. Y. Yu, H. Y. Lin and R. N. Lin, *Eight-scale image contrast enhancement based on adaptive inverse hyperbolic*, International Symposium on Computer, Consumer and Control, Taichung, Taiwan, (2014), 98-102.

[18] C. Y. Yu, H. Y. Lin, Y. C. Ouyang and T. W. Yu, *Modulated AIHT image contrast enhancement algorithm based on contrast-limited adaptive histogram equalization*, International Journal on Applied Mathematics and Information Sciences, **7(**2) (2013), 449-454.

[19] C. Y. Yu, Y. C. Ouyang, C. M. Wang and C. I. Chang, *Adaptive inverse hyperbolic tangent algorithm for dynamic contrast adjustment in displaying scenes*, EURASIP Journal on Advances in Signal Processing, **485151** (2010), 1-20.

[20] J. Yue, J. Liu, X. Liu and W. Tan, *Identification of nonlinear system based on ANFIS with subtractive clustering*, The Sixth World Congress on Intelligent Control and Automation (WCICA 2006), 2006, 1852-1856.

[21] K. Zuiderveld, *Contrast limited adaptive histogram equalization*, In: P. Heckbert: Graphics Gems IV, Academic Press 1994.

Sheng-Chih Yang, Department of Computer Science and Information Engineering, National Chin-Yi University of Technology, Taichung City 411, Taiwan, ROC
E-mail address: scyang@ncut.edu.tw

Cheng-Jian Lin*, Department of Computer Science and Information Engineering, National Chin-Yi University of Technology, Taichung City 411, Taiwan, ROC
E-mail address: cjlin@ncut.edu.tw

Hsueh-Yi Lin, Department of Computer Science and Information Engineering, National Chin-Yi University of Technology, Taichung City 411, Taiwan, ROC
E-mail address: hyl@ncut.edu.tw

Jyun-Guo Wang, Department of Computer Science and Information Engineering, National Chin-Yi University of Technology, Taichung City 411, Taiwan, ROC
E-mail address: jyunguo.wang@gmail.com

Cheng-Yi Yu, Department of Computer Science and Information Engineering, National Chin-Yi University of Technology, Taichung City 411, Taiwan, ROC
E-mail address: youjy@ncut.edu.tw

∗Corresponding author